Residential Solar Cell System by driving of High Efficiency Inverter

Kwak Dong-Kurl
Department of Electrical Engineering
Donghae University, Kangwondo, Korea
dkkwak@mail.donghae.ac.kr

Lee Hyun-Woo
Division of Electrical and Electronic Engineering
Kyungnam University, Kyungnam, Korea
lhwoo@kyungnam.ac.kr

Abstract : With today's global environmental and energy problems, high expectations exist for solar power generation to reduce carbon dioxide generated by the consumption of fossil fuels. On the other hand, power consumption in residential homes is increasing every year. Among the many household appliances, the power demand for air conditioners increases dramatically during the summer, particularly in the afternoons. As this pattern closely matches the output pattern of solar cells, it should be possible to combine a photovoltaic array with an air conditioner to decrease the energy consumption within the home. We have developed a residential solar-powered air conditioner that operates through a combination of photovoltaic array and commercial power. In this paper, the configuration and specification of the residential solar-powered system are described to a novel high efficiency inverter using a ZVCS boost converter. And the performance evaluations of the solar-powered air conditioner are examined by the analysis of a new tracking controller with a maximum power P_{max} detection of solar cell.

Key words : Solar cell, inverter air conditioner, partial resonant method, P_{max} tracking controller.

1. Introduction

The solar radiation has an irregularly varying factor due to a basic day and night cycle and climatic conditions. As this condition closely matches the output condition of solar cells, it should be possible to combine a photovoltaic array with a residential solar-powered system to decrease the energy consumption within the home. We have developed a residential solar-powered air conditioner that operates through a combination of photovoltaic array and commercial power, as shown in Fig. 1. A solar cell has an optimal operating point to be able to get the maximum power P_{max}. So, many P_{max} tracking controllers using the line voltage of a solar cell have been popularly used [1],[2]. But it may vary depending on the miss match between the solar cell output and the load. We investigate the possibilities of P_{max} control using the reactor current tracking control instead of the line voltage of solar cell in order to solve the point at issue above [3].

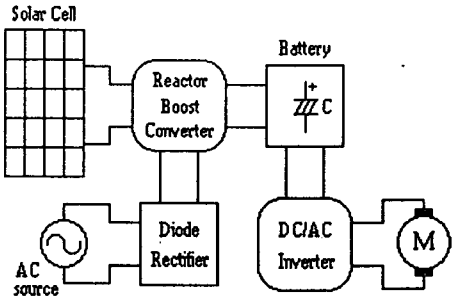

Fig. 1. Block diagram of solar-powered system

And we have developed a residential solar cell by driving of a high efficiency dc-ac inverter that operates through a combination of photovoltaic array and commercial power. The inverter is operated with matching a ZVCS boost converter by the partial resonant method [4].

2. System configuration and Analysis

2.1 System configuration

Fig. 2 shows a configuration of solar cell system of dispersion type with system interconnection that applies an inverter air conditioner, that is, solar-power air conditioner. The solar cell system is designed to have no effect on reverse power flow in power system.

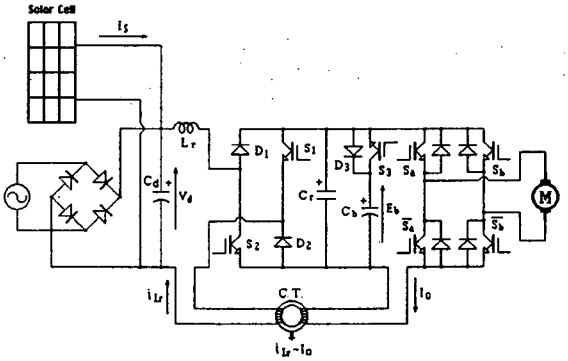

Fig. 2. Configuration of the solar-powered air conditioner by driving of high efficiency inverter

In order to be useful for the solar cell, the system requires that the solar cell generation power matches a pattern of output load. The reactor boost converter and dc-ac inverter using power conversion system are operated a high efficiency and high power factor. The switching devices in the proposed conversion systems are operated with soft switching by the partial resonant method. The partial resonant circuit makes use of a reactor using step up and a condenser of loss-less snubber.

2.2 High efficiency Inverter for ZVCS boost converter

The control switches in a power converter are subjected to high switching power losses and switching stresses. As a result of those, the power system bring on a low efficiency. To improved these, a large number of soft switching topologies included a resonant circuit has been proposed. But these circuits increase number of switch in circuit and complicate sequence of switching operation. Therefore authors propose that a novel soft switching converter by a partial resonant circuit. The partial resonant operation makes zero current switching(ZCS) and zero voltage switching(ZVS) for the control switches without switching power losses. The results are that the switching loss is very low and the efficiency of system is high. Also the circuit has a merit which is taken to more increase of efficiency, as it makes to a regeneration at the input source of an accumulated energy in snubber condenser without loss of snubber in conventional circuit. Fig. 3 shows equivalent circuits of operating modes in one cycle switching.

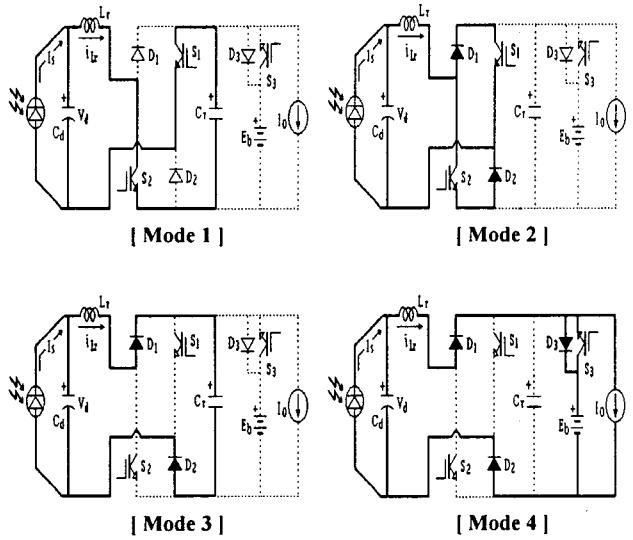

Fig. 3. Equivalent circuits of operating modes in one cycle switching

At initial condition, the current flowing through the reactor L_r is zero. The switch S_1 and S_2 are off-state, S_3 is on-state and condenser C_r is charged at the same voltage of dc output voltage E_b. The simulated waveforms for the proposed inverter using ZVCS boost converter are shown in Fig. 4.

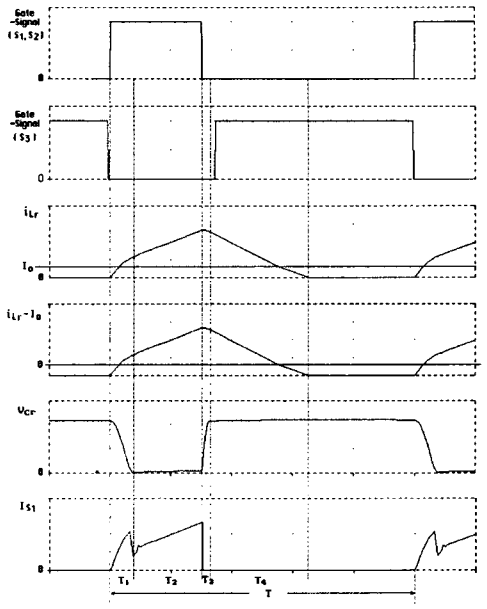

Fig. 4. Simulation waveforms for switching operation

MODE 1 : T_1

Mode 1 begins by turning on both switch S_1 and S_2, and S_3 is turn-off at the same time. This mode takes form of LC resonance circuit with a circuit path of V_d+-L_r-S_2-C_r-S_1-V_d-. Then the input dc voltage V_d and the voltage v_{cr} of condenser C_r are added and applied to the reactor L_r. Turn-on of the switch S_1 and S_2 occurs in zero current state, and the switch S_3 is driven zero voltage switching. This mode ends when v_{cr}=0.

MODE 2 : T_2

Mode 2 begins when the voltage of across C_r achieves zero. Then diodes D_1 and D_2 start conduction. The reactor current i_{Lr} is divided into two short circuit paths of S_1-D_1 and S_2-D_2. The reactor current is linearly increased by this mode. The switches S_a~S_b of the inverter part are transfered to switching by the zero voltage at this mode.

MODE 3 : T_3

Mode 3 begins by turning off both S_1 and S_2 at the same time. The reactor current takes a route of D_1-C_r-D_2 and charges C_r. Then this mode takes form of LC resonance circuit. Turn-off of S_1 and S_2 occurs in ZVS, because the voltage of C_r is zero voltage. $v_{cr}=E_b$ is achieved and the

diode D_3 is begun to conduct, then this mode ends.

MODE 4 : T_4

Mode 4 begins when the voltage of across C_r achieves output voltage E_b. The reactor current i_{Lr} flows into the load. The reactor current is decreased and achieved to zero at the end of mode 4. When the diode D_3 is begun to conduct, the switch S_3 is turned on ZVS.

2.3 Steady-state Analysis and P_{max} tracking controller

The proposed circuit is analyzed to steady-state by a state averaging method. Where, (a) The resonant period is shorter than the switching period. (b) Each device using circuit regards as ideal one. Therefore, each state equation can be represented as

$$\frac{d\,i_{Lr}}{d\,t} = i'_{Lr}, \quad \frac{d\,V_d}{d\,t} = V'_d$$

From the equivalent circuit of mode 2, we can write the following state equation.

$$\begin{bmatrix} i'_{Lr} \\ V'_d \end{bmatrix} = \begin{bmatrix} 0 & \frac{1}{L_r} \\ -\frac{1}{C_d} & 0 \end{bmatrix} \begin{bmatrix} i_{Lr} \\ V_d \end{bmatrix} + \begin{bmatrix} 0 \\ \frac{I_S + I_o}{C_d} \end{bmatrix} \quad (1)$$

And the following state equation can be written by the equivalent circuit of mode 4.

$$\begin{bmatrix} i'_{Lr} \\ V'_d \end{bmatrix} = \begin{bmatrix} 0 & 0 \\ 0 & 0 \end{bmatrix} \begin{bmatrix} i_{Lr} \\ V_d \end{bmatrix} + \begin{bmatrix} -\frac{E_b}{L_r} \\ \frac{I_S}{C_d} \end{bmatrix} \quad (2)$$

Where the switching duty factor D of mode 2 and mode 4 puts in $D = T_{on}/T$ (T:switching period, T_{on}:switching turn on period). Each state equation is given as

$$\begin{bmatrix} i'_{Lr} \\ V'_d \end{bmatrix} = \begin{bmatrix} 0 & \frac{D}{L_r} \\ -\frac{D}{C_d} & 0 \end{bmatrix} \begin{bmatrix} i_{Lr} \\ V_d \end{bmatrix} + \begin{bmatrix} -\frac{E_b(1-D)}{L_r} \\ \frac{I_S + D\,I_o}{C_d} \end{bmatrix} \quad (3)$$

and V'_d, i'_{Lr} at steady-state is zero. Therefore, the reactor current i_{Lr} is expressed as follows

$$i_{Lr} = I_{av} = I_o + \frac{I_S}{D} \quad (4)$$

where I_{av} is average value of the reactor current i_{Lr}. From stated equations above, the correlation between V_d and E_b is

$$V_d = \frac{1-D}{D} E_b \quad (5)$$

From the equation (4),

$$\begin{aligned} I_{av} &= I_o + \left(1 + \frac{V_d}{E_b}\right) I_S \\ &= I_o + \left(I_S + \frac{Solar\ output\ power}{E_b} \right) \end{aligned} \quad (6)$$

where the difference between reactor current i_{Lr} and output current I_o, $i_{Lr} - I_o$ is detected by current transformer C.T. The average value I^*_{av}, that is, I^*_{av} = average $I_{av} - I_o$ is

$$\begin{aligned} I^*_{av} &= \left(1 + \frac{V_d}{E_b}\right) I_S \\ &= \left(I_S + \frac{Solar\ output\ power}{E_b} \right) \end{aligned} \quad (7)$$

Therefore we find out that the line voltage V_d of a solar cell is controlled by duty factor D of switch S_1, S_2. When the input power P_{in} of battery is gotten to maximum, the output power of solar cell is generated with P_{max}. The charging period of battery occurs in turn-off period of switch S_1 and S_2, as shown in Fig. 5. Therefore the input power P_{in} is represented as

$$\begin{aligned} P_{in} &= \frac{E_b}{T} \int_0^{T_{iL0}} \left(-\frac{E_b}{L_r} t + I_{LH} \right) dt \\ &= \frac{D\,E_b}{T_{on}} \left(-\frac{E_b}{2L_r} T_{iL0}{}^2 + I_{LH}\, T_{iL0} \right) \end{aligned} \quad (8)$$

where

$T_{on} = L_r\,\Delta I_L / V_d$, $T_{iL0} = L_r\,\Delta I_L / E_b$, $\Delta I_L = I_{LH} - I_{LL}$,

$I_{av}^{*}=\frac{1}{2}(I_{LH}+I_{LL})$. Then, the equation is expressed as follows

$$P_{in} = D \cdot I_{av}^{*} \cdot V_d = (1-D) \cdot I_{av}^{*} \cdot E_b \qquad (9)$$

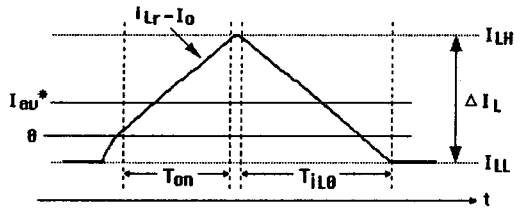

Fig. 5. Detecting waveform of C.T

and multiplied equation (7) by $(1-D) \cdot E_b$, input power is

$$(1-D) \cdot I_{av}^{*} \cdot E_b = V_d \cdot I_S \qquad (10)$$
$$(Solar\ output\ power)$$

Therefore, When the input power P_{in} of battery is gotten to maximum, the output power of solar cell is generated with maximum power. Active operation of $(1-D) \cdot I_{av}^{*}$ is simple from analog RC filter, as shown in Fig. 6.

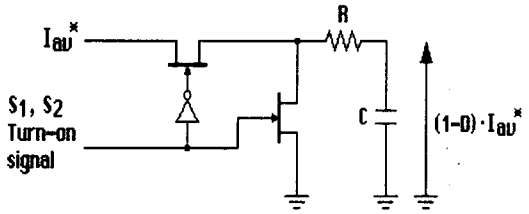

Fig. 6. Operational circuit of $(1-D) \cdot I_{av}^{*}$

When the switch S_1 and S_2 is turn-off, I_{av}^{*} charges condenser C. But turn-on, the voltage of C is recharged by R. Therefore, $(1-D) \cdot I_{av}^{*}$ can be detected from the tracking of the condenser voltage.

3. Performance evaluations and Experimental results

Table 1 shows the specification of components using in experiment circuit of the solar-powered air conditioner. Fig. 7(a) (case 1: battery voltage 120[V]) and Fig. 7(b) (case 2: battery voltage 240[V]) are represented to I_{av}^{*}, $(1-D) \cdot I_{av}^{*}$ and solar cell output power P compared with the line voltage of solar cell module.

Table 1 Specification of the solar-powered air conditioner

Solar Cell	Maximum output power (W)	550
	Optimal operation Voltage (V)	100
Boost converter	Input voltage (V)	100
	Output voltage (V)	120~320
	Efficiency (%)	96
Air conditioner	Rated output (kW)	Cool air : 2.0 (0.2~2.5)
		Hot air : 3.0 (0.1~3.7)
	Consumed power (kW)	Cool air : 1.0 (0.1~1.2)
		Hot air : 1.2 (0.08~1.3)

Each peak point is in accord with one of solar cell output power. This shows that I_{av}^{*} has no effect on variety of I_S.

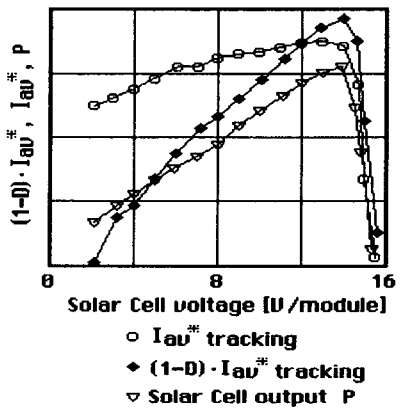

(a) Case 1

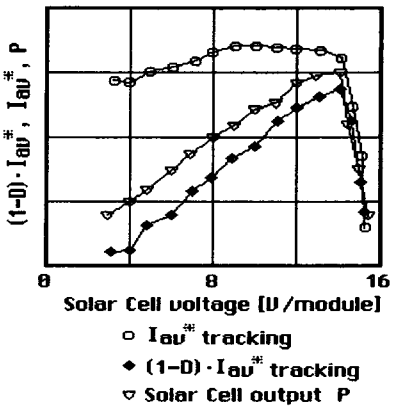

(b) Case 2

Fig. 7. Performance evaluations of solar cell

Fig. 8 shows performance evaluations of calculating value and measuring value on (a) cool air operation and (b) hot air operation. In case of cool air operation, a setting temperature of air conditioner is 27℃. In case of hot air operation, that is 20℃.

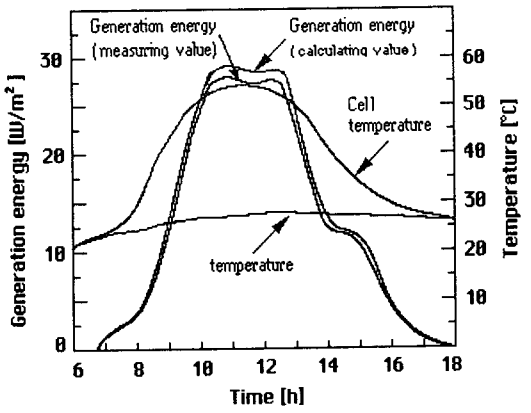

(a) cool air operation

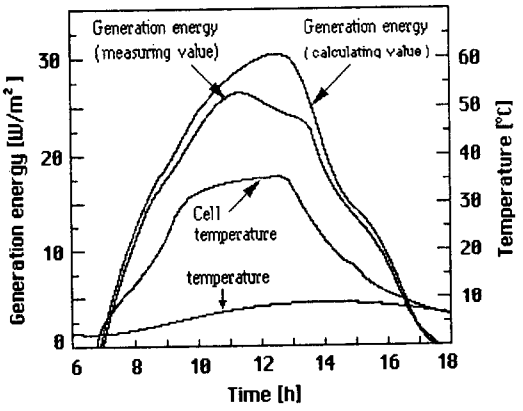

(b) hot air operation

Fig. 8. Operation characteristic of solar-power air conditioner

The result is that the measuring value of solar cell generation energy is in accord with the calculating value of that. The utilization fator η of solar-powered air conditioner at a day is calculated as follows

$$\eta = (P_m / P_c) \times 100 \ [\%] \qquad (11)$$

where P_m is the measuring value of solar cell generation energy and P_c is the calculating value of that. P_m=110 [Wh/m²], P_c=117 [Wh/m²] from Fig. 8(a), therefore, η= 94.0 [%] . Also P_m=182 [Wh/m²], P_c=203 [Wh/m²] from Fig. 8(b), therefore, η= 89.6 [%] . In case of Fig. 8(b), the measuring value of generation energy is limited because the rise in temperature is occured to decrease in the load. The result is that the utilization fator is decreased. The experimental results are included to confirm the validity of the analytical results.

4. Conclusion

In this paper, the configuration and specification of the residential solar-powered system were described to a novel high efficiency inverter using a ZVCS boost converter. The switching devices in the proposed conversion systems were operated with soft switching by the partial resonant method. The partial resonant circuit made use of a reactor using step up and a condenser of loss-less snubber. And the performance evaluations of the solar-powered air conditioner were examined by the analysis of $(1-D)\cdot I_{av}^{*}$ tracking controller with a maximum power P_{max} detection of solar cell. Active operation of $(1-D)\cdot I_{av}^{*}$ was simple from analog RC filter. The results were that the switching loss was very low and the efficiency of system was high.

References

[1] Tokuo, Shigeo, "Comparisons of Maximum Power Tracking Strategy of Solar Cell Output and Control Characteristics using Step up/down Chopper Circuit", T.IEE Japan, Vol. 112-D, No. 3, pp250-257, 1992

[2] Katsumi, Iwao, "A New Maximum Power Tracking Method of Photovoltaic Power Generator Taking Frequency Characteristics of Solar Cell Module into Consideration", T.IEE Japan, Vol. 112-D , No. 3, pp258-263, 1992

[3] Kwak D.K, Lee H.W, "Maximum power tracking Strategy of a Solar Cell using ZVCS converter", KIEE summer conf., pp1032-1034, 2001. 7

[4] Kwak D.K, Lee H.W, "High Power Buck-Boost DC-DC Converter of Soft Switching for Photovoltaic Power Generation", KIPE conf., pp117-120, 1996. 6